# Morphological Fractal Dimension Versus Power-law Exponent in the Scaling of Damaged Media

ALBERTO CARPINTERI,* GIUSEPPE LACIDOGNA, GIANNI NICCOLINI AND SIMONE PUZZI

*Politecnico di Torino, Department of Structural Engineering & Geotechnics, Corso Duca degli Abruzzi 24 – 10129 Torino, Italy*

**ABSTRACT:** Fractal Geometry has been widely used for the description of irregular phenomena in various scientific fields recently. In the subjects concerning fracture system characterization, fractals represent the fracture surfaces in two or 3D problems. In the last few years the fractal geometry of crack networks in damaged materials has been statistically characterized by two power laws, respectively, describing the spatial distribution of crack barycenters, and the crack length distribution. In this article, we explore the potential of the latter power-law. Merely using such statistical model to describe the population of cracks, besides providing a theoretical basis for explaining lower limits to the *b*-value both in seismicity and in acoustic emission (AE) tests, we find a simple relation between *b* and the fractal dimension *D* of the crack network. As a result, the *b*-value analysis in AE monitoring tests permits evaluation of the dimension *D* of the damaged domain. This method of evaluating *D* is herein applied to a concrete specimen in compression, subjected to AE monitoring, loaded up to failure. In this test, the characterization of the fracture process through analysis of AE signals emerging from the growing cracks has been performed in a post-processing environment, using two different procedures. In fact, besides the two-point correlation algorithm introduced by Grassberger and Procaccia, the damage process has been evaluated through the *b*-value analysis. Both procedures make it possible to evaluate the dimension *D* of the damaged domain, i.e., the fractal dimension of the crack network. The obtained results are consistent with our understanding of damage phenomenon.

**KEY WORDS:** crack size distribution, fractal dimension, acoustic emission, concrete structures, damage mechanics.

*Author to whom correspondence should be addressed. E-mail: alberto.carpinteri@polito.it
Figures 7–12 appear in color online: http://ijd.sagepub.com



1056-7895/09/03 259–24 $10.00/0 DOI: 10.1177/1056789508098700

Los Angeles, London, New Delhi and Singapore

## INTRODUCTION

THE MANNER IN which fracture system properties at different scales relate to each other, i.e., their scaling properties, has become an active field of research in the last 30 years, motivated by the promise of statistical prediction that scaling laws offer. Power laws are recognized to provide a key in earthquake hazard assessment, in hydrocarbon reservoir management, and in hazardous waste disposal. Power law distributions are clearly scale invariant. The idea of the scale invariance is that the ratios between different scales are preserved. One of the first inklings of scale invariance in Fracture Mechanics came from the observation of the Gutenberg–Richter (GR) law for earthquakes (Turcotte, 1997), $N(\geq A) \propto A^{-b}$, where $N$ is the number of earthquakes with source rupture area $\geq A$, and typically $b \approx 1$: for each earthquake with source rupture area $\geq A_0$, there are 10 earthquakes with area $\geq A_0/10$, 100 with area $\geq A_0/100$, and so forth.

Fractal Geometry has been widely used for the description of irregular phenomena in various scientific fields recently. In the subjects concerning fracture system characterization, fractals represent the fracture surfaces in 2 or 3D problems. On the other hand, fractal geometry is not only useful to study complex shapes, but also it may be a powerful tool for a geometric characterization of microcrack networks by using fractals with 'dust-like' structure such as the Cantor set. Statistical characteristics of such damage phenomena in disordered materials (i.e., random position, size, and orientation of the microcracks) may be taken into account adopting random fractals. The scale invariance is a peculiarity of fractal objects.

In recent years, the term 'fractal'– coined by Mandelbrot (1982) from the Latin *fractus*, meaning broken, to describe objects that were too irregular to fit into a traditional geometrical setting – has been widely used to describe any kind of fracture feature following a power-law distribution, such as size, displacement, and aperture distributions. Hence, the question that can be addressed is whether a fracture network, whose crack length distribution exhibits a power-law behavior describes a morphologic fractal (Turcotte, 1997; Bonnet et al., 2001).

A simple theoretical model of fragmentation, where all scales are involved during crack growth with repetitive subdivision of breakage patterns, was originally proposed in the 1980's (King, 1986; Sammis et al., 1986; Turcotte, 1986). Known in Physics as the Apollonian model, it gives rise to a power-law size distribution, whose exponent was equated to the fractal dimension of the system (Hausdorff, 1919). As a matter of fact, for about 15 years this model remained the only theoretical support for a fractal description of crack pattern geometry, since the relation between the crack length exponent and the fractal dimension was poorly investigated. Conversely, a very

interesting application of the fractal framework to the modeling of damage of brittle 2D lattices has been recently proposed (Krajcinovic and Rinaldi, 2005; Rinaldi et al., 2006); in this statistical damage mechanics approach, the connection between damaged random heterogeneous micromaterial and the system macroparameter is sought. The fractal dimension is used to investigate the transition between damage nucleation and propagation and to propose constitutive relations and scaling laws. In this paper, we investigate a similar topic, aiming at establishing a simple relation between the fractal dimension $D$ of crack barycenters and the exponent $\gamma$ of the power law crack length distribution.

In the last few years, a relation $D=\gamma/x$ linking these two quantities has been introduced (Bonnet et al., 2001; Bour and Davy, 1999; Bour et al., 2002), where $x$ is the exponent relating the average distance $d(L)$ from the center of a crack having length $L$ to its nearest neighbor of larger length. The previously mentioned relation (which agrees with the fragmentation model in the particular case $x=1$) derives from three scaling laws assumed for describing fractal features of a crack network, $N_{TOT} \propto s^D$ giving the number $N_{TOT}$ of cracks observed within a volume of characteristic linear size $s$, $N(\geq L) \propto L^{-\gamma}$ for the number of cracks with length $\geq L$, and $d(L) \propto L^x$ for the spatial correlation and organization between cracks (Turcotte, 1997; Bonnet et al., 2001; Bour and Davy, 1999; Bour et al., 2002).

Since the 1980's the power-law crack length distribution $L^{-\gamma}$ has been drawn under the well-founded hypothesis that the larger the body, the larger the maximum crack inside it (Carpinteri, 1986, 1989, 1994a). Besides providing a theoretical basis for explaining lower limits to the so-called '$b$-value' of the GR law for earthquake and AE statistics (Carpinteri et al., 2006a), this crack length distribution seems intrinsically to account for fractal morphology of crack networks without need of any further *ad hoc* assumptions.

An experimental evidence of this phenomenon can be obtained by applying the Acoustic Emission (AE) technique to materials experiencing damage (Ohtsu, 1996; Colombo et al., 2003; Carpinteri et al., 2006a,b). In fact, the exponent $b$ of the GR law $N(\geq A) \propto A^{-b}$ (where $A$ is the amplitude of AE signals) changes with the different stages of damage growth. The initially dominant microcracking generates a large number of low-amplitude AE signals (which are proportional to their source rupture surfaces), while the following macrocracking generates less signals but of higher amplitude. This implies a progressive decrease of the $b$-value as the specimen approaches impending failure: this is the core of the $b$-value analysis used for damage assessment.

On the other hand, the damage process is also characterized by its progressive localization: at its early stage, damage consists of a myriad of

microcracks chaotically distributed over a large part of the specimen volume, while at the final stage microcracks coalesce to form the through-going fracture surface. In geometric words, the dimension $D$ of the damaged domain is expected to decrease from an initial value comprised between 2 and 3 (which is the maximum value since the the fractal dimension of a fractal object cannot exceed the geometric dimension of the support, in this case the 3D Euclidean space) towards a final value nearly equal to 2. Therefore, both parameters $b$ and $D$ share a decreasing trend as the damage develops.

Adopting only the above-mentioned crack length distribution to describe a population of cracks and regarding such cracks as sources of AE activity, we establish a simple relation between $b$ and $D$. In this way, we propose a method of characterizing the spatial distribution of damage through the AE technique avoiding time-consuming location of the cracks.

## SPATIAL AND LENGTH DISTRIBUTIONS OF MICROCRACK NETWORKS

### Background

Fractal distributions for particle-size distributions are observed in nature for a variety of fragmented objects:

$$N(\geq L) = CL^{-\gamma}, \tag{1}$$

where $N(\geq L)$ is the number of fragments with a characteristic linear dimension greater than $L$ and $C$ is a constant chosen to fit the observed distributions (Turcotte, 1997). Here the term fractal stands for fractional and it is widely referred to the exponent $\gamma$, generally not integer, of any kind of statistical power-law distribution even if not directly associated with a fractal morphology. A simple theoretical model of fragmentation, where all scales are involved during crack growth with repetitive subdivision of breakage patterns, see Figure 1, was originally proposed in the 1980's (Sammis et al., 1986) in order to explain observed fractal distributions of rock fragments in crustal shear zones at the plates' boundaries (King, 1986; Davy et al., 1990).

This model, known in Physics as the Apollonian model discussed and supported by laboratory observations in Sammis and Steacy (1995), is based on the hypothesis that the fracture probability is maximum for neighboring fragments of the same size, while it is unlikely that small fragments will break large fragments or that large fragments will break

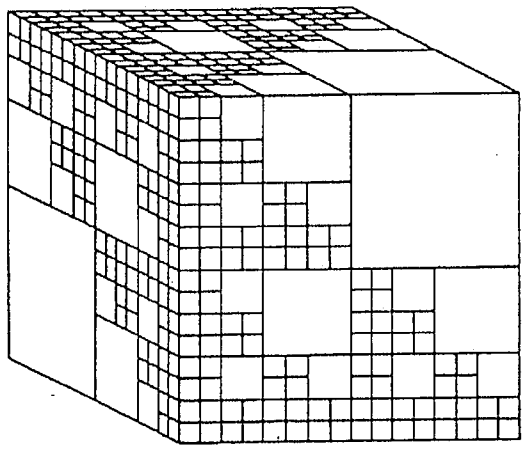

***Figure 1.*** *Illustration of a deterministic fractal model for fragmentation (Apollonian model). Two diagonally opposite cubes are retained at each scale (Sammis et al., 1986).*

small fragments. In this model, fragmentation begins at the scale of largest fragments, since they are the weakest, and continues with a cascade of fragmentation at progressively smaller scales, leading to a fractal distribution of crushed material. For the configuration illustrated in Figure 1 an initially intact cube with a linear dimension $h$ is fragmented in $N_1 = 2$ blocks with size $r_1 = h/2$, $N_2 = 12$ with $r_2 = h/4$, and $N_3 = 72$ with $r_3 = h/8$. The dimension $D$ of this deterministic fractal, defined as (Turcotte, 1997):

$$D = \frac{\ln(N_{n+1}/N_n)}{\ln(L_n/L_{n+1})}, \tag{2}$$

being $N_n$ the number of fragments with linear dimension $L_n$ and $N_{n+1}$ the number of immediately smaller fragments, is $D = \ln 6/\ln 2 = 2.58$. The cumulative number of blocks larger than a specified size for the three highest orders are $N_{1C}(\geq r_1) = 2$ for $r_1 = h/2$, $N_{2C}(\geq r_2) = 14$ for $r_2 = h/4$, and $N_{3C}(\geq r_3) = 86$ for $r_2 = h/8$. The cumulative statistics for this model is in excellent agreement with the power-law Equation (1) for $\gamma = 2.60$. Thus, in this fragmentation model the fractal dimension $D$ is nearly equal to the exponent $\gamma$ of the cumulative length distribution (Turcotte, 1997):

$$D \cong \gamma \tag{3}$$

This model of fragmentation remained for several years the only theoretical support to connect the fractal dimension $D$ of the spatial distribution of microcracks to the exponent $\gamma$ of the frequency length distribution of microcracks. In this case $N(\geq L)$ stands for the number of microcrack

advancements larger than $L$ in the crack network (Carpinteri et al., 2004, 2006b).

More recently, three scaling-laws were assumed in order to provide a statistical description of the basic features of crack networks. For a population of cracks, the manner in which the number of cracks decreases with size was assumed to follow a power-law behavior, and then the number $N(\geq L)$ of microcracks larger than $L$ is given again by (Bour and Davy, 1999; Bonnet et al., 2001; Bour et al., 2002):

$$N(\geq L) \propto L^{-\gamma}. \tag{4}$$

Crack positions were defined from the crack barycenters, whose spatial distribution was assumed to be fractal with dimension $D$. According to Mandelbrot (1982), this means that the number of microcracks embedded in a volume of linear size $s$ increases with $s$ such as (Bour and Davy, 1999):

$$N(s) \propto s^{D}. \tag{5}$$

Various operative methods exist to find the box dimension $D$ of a system (Falconer, 1990). Here, the minimum number $N(d)$ of balls of radius $d$ necessary for covering the microcrack net was taken (Bour and Davy, 1999). In the limit of small $d$, such number scales as:

$$N(d) \propto \left(\frac{s}{d}\right)^{D}. \tag{6}$$

For mathematical sets $D$ is defined when $d$ tends to zero. In practice, for natural systems the lower cut-off scale $d$ of the relationship is the distance between the elements constituting the system. In the case of a microcrack network the lower limit for $d$ is the size of the grains. Even, there exists an upper cut-off, given by the size and shape of a given specimen.

A modified box-counting method was proposed by Bour and Davy (1999), in which the lower cut-off scale is the average distance $d(L)$ between a crack of length $L$ and its nearest neighbor of length $\geq L$. The distance is calculated between the crack barycenters. This method assumes that any subset of the crack barycenters, i.e., neglecting cracks $<L$, remains fractal. The idea is that the number of balls necessary to cover the set will be equal to the number $N(\geq L)$ of sampled points if the ball radius is $d(L)$. Following Equation (6), the number of sampled points should scale with the distance between nearest points as:

$$N(\geq L) \propto \left(\frac{s}{d(L)}\right)^{D} \tag{7}$$

Since the crack length distribution is assumed to be a power law, Equations (4) and (7) predict $d(L)$ to scale as (Bour and Davy, 1999; Bonnet et al., 2001; Bour et al., 2002):

$$d(L) \propto L^x, \tag{8}$$

with:

$$x = \frac{\gamma}{D}. \tag{9}$$

The third scaling law given by Equation (8) describes the spatial organization of a microcrack network: the longer cracks are more mutually separated than the shorter. Therefore, according to Bour and Davy (1999) the fractal dimension $D$ and the length exponent $\gamma$ are related through the relation of Equation (9), where $x$ is the exponent relating the average distance from a crack to its nearest neighbor of larger length. It can be noted that the case of $\gamma = D$ in the fragmentation model corresponds to the self-similar case $x = 1$ (Bonnet et al., 2001).

**From Self-affinities to Power-law Distributions**

In Damage Mechanics, the distribution of microcracks in disordered materials can be statistically approached by defining a probability density function $p'(L, \vartheta, \varphi)$, $L$, $\varphi$, and $\vartheta$ being, respectively, the size of the microcrack, the longitude, and the latitude of its orientation (Carpinteri, 1986, 1989, 1994a; Krajcinovic, 1996; Carpinteri et al., 2006a).

For the sake of simplicity, the spatial distribution of cracks is assumed to be uniform over a fractal domain of dimension $2 \leq D \leq 3$, where cracks positions are given by their barycenters. As already remarked, the fractal dimension $D$ cannot exceed the geometric dimension of the support, which is equal to 3 (in case of a 3D Euclidean space). Furthermore, assuming that the distribution of microcracks for concrete-like materials is isotropic, i.e., $p'(L, \vartheta, \varphi) = p'(L)$, the probability density will take the form (Carpinteri, 1986, 1989, 1994a; Carpinteri et al., 2006a):

$$p'(L, \vartheta, \varphi) = \frac{p(L)}{4\pi}, \tag{10}$$

being $p(L)$ the probability density of microcrack size distribution, since all orientations are alike.

Now, let us consider a body of characteristic linear size $s$; we can compute the value $\overline{L}$ of the crack size, such that, on average, one defect only (i.e., the largest) exceeds it. Let the cracking in the body be uniform, so that we may

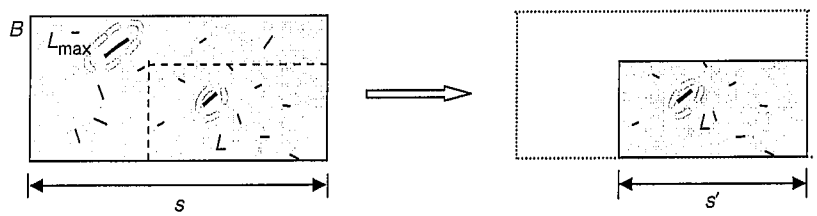


***Figure 2.*** *In a portion s' given by solving the equation $(s'/s)^{\delta} = L/L_{max}$ the defect of size L can be statistically considered as the largest defect.*

define $\rho$ as the mean fractal density of microcrack barycenters. Hence, the following relation holds:

$$1 = \Pr[L \geq \overline{L}]\rho s^D \frac{1}{4\pi}\int_0^{2\pi}\int_0^{\pi} \sin\vartheta \, d\vartheta \, d\varphi. \tag{11}$$

where Pr[X] is the probability of the event X to occur. It is of interest the particular distribution $p(L)$ for which the maximum crack size $L_{max}$ in a body is proportional to the linear size $s$ of the body itself, $L_{max} \propto s^{\delta}$, the condition $\delta = 1$ representing the case of perfect self-similarity, whereas, in general, $\delta$ can be different from 1, entailing simply self-affinity (Figure 2).

Assuming this hypothesis, if a geometrically similar body of characteristic linear size $ks$ is considered, we impose that one defect only exceeds the threshold $k^{\delta}\overline{L}$; it is thus possible to write:

$$1 = \Pr[L \geq k^{\delta}\overline{L}]\rho(ks)^D \frac{1}{4\pi}\int_0^{2\pi}\int_0^{\pi} \sin\vartheta \, d\vartheta \, d\varphi. \tag{12}$$

Equating the right-hand terms of Equations (11) and (12) we readily obtain:

$$\Pr[L \geq k^{\delta}\overline{L}]k^D = \Pr[L \geq \overline{L}]. \tag{13}$$

The solution of Equation (13) is (Carpinteri, 1986, 1989, 1994a; Carpinteri et al., 2006a):

$$P(L) = 1 - \frac{1}{\gamma}\frac{c_0}{L^{\gamma}}, \quad \forall L > L_0, \tag{14}$$

being $c_0$ a constant of proportionality and $P(L)$ the cumulative probability. By derivation, we obtain the following probability density function:

$$p(L) = \frac{c_0}{L^{\gamma+1}}, \quad \forall L > L_0, \tag{15}$$

and:

$$\gamma \equiv \frac{D}{\delta}. \tag{16}$$

It can be observed that $L_{\max}$ is, in a body of size $ks$, a random value exceeding the threshold $k^{\delta}\overline{L}$, and now we also know that $L$ is distributed according to the probability density function of Equation (15). Therefore, we can compute its expected value. The result shows that it is proportional to the threshold $k^{\delta}\overline{L}$ itself:

$$E\left(L \middle| L \geq k^{\delta}\overline{L}\right) = \frac{\int_{k^{\delta}\overline{L}}^{+\infty} L\, p(L)\mathrm{d}L}{\int_{k^{\delta}\overline{L}}^{+\infty} p(L)\mathrm{d}L} = \frac{\gamma - 1}{\gamma - 2} k^{\delta}\overline{L}, \tag{17}$$

Thus, Equation (15) implies the self-affinity relation to hold: $L_{\max}(s) \propto s^{\delta}$, and *vice versa*; this result is also confirmed by Newman (2005), who writes a similar relation linking the maximum size $L_{\max}$ with the number of samples from a distribution of the form of Equation (15). This distribution can be referred to as the crack size distribution of self-affinity. Comparing Equations (6) and (9), it can be noted that $\delta = x^{-1}$; the exponent $\delta$ characterizing the scaling of the maximum crack size with the structural size $s$ is thus the reciprocal of the exponent $x$ introduced by Bour and Davy (1999); the implications will be discussed in the forthcoming sections.

**Power-law Crack Size Distributions and Gutenberg–Richter Law**

Microcracks are now considered as sources of AE activity. It is widely accepted a fractal interpretation of GR law, initially drawn in seismicity (Aki, 1981; Turcotte, 1997), which says how AE events generated by source cracks statistically distribute (Sammonds et al., 1994; Ohtsu, 1996; Colombo et al., 2003; Rao and Lakshmi, 2005; Carpinteri et al., 2006a):

$$N(\geq L) \propto L^{-2b}, \tag{18}$$

where $N$ the number of AE events generated by source microcracks with a characteristic linear dimension $\geq L$, and $b$ is a parameter which says how large the ratio of events with low magnitude (i.e., smaller microcracks) to larger ones (that is with higher magnitude) is. On the other hand, the number of cracks with length $\geq L$ expected from the distribution of Equation (14) is (Carpinteri et al., 2006a):

$$N(\geq L) \propto L^{-\gamma}. \tag{19}$$

Equating the cumulative distributions of Equations (18) and (19) gives (Carpinteri et al., 2006a; Carpinteri et al., 2007):

$$\gamma = 2b. \tag{20}$$

From the literature on AE tests, it is well-known that the $b$-value decreases as the specimen approaches impending failure (Sammonds et al., 1994; Ohtsu, 1996; Colombo et al., 2003; Rao and Lakshmi, 2005; Carpinteri et al., 2006a; Carpinteri et al., 2007). It is common to observe a trend of $b$ to the critical value $b_{crit}=1$ during final crack propagation (Colombo et al., 2003; Rao and Lakshmi, 2005; Carpinteri et al., 2006a; Carpinteri et al., 2007). A theoretical basis for explaining $b_{crit}=1$ can be established, by exploiting properties of the distribution of self-affinity given by Equation (23) (Carpinteri et al., 2006a). Substituting Equation (28) into Equation (24) we obtain the following expression for $b$:

$$b \equiv \frac{D}{2\delta}. \tag{21}$$

The minimum of the $b$-value is obtained when $D=2$ and $\delta=1$ and it is thus equal to 1. In fact, $L_{max}(s) \propto s^{\delta}$ is equivalent to the following relations:

$$s(k) \propto k, \tag{22}$$

$$L_{max}(k) \propto k^{\delta}, \tag{23}$$

where $k$ is a dimensionless scaling factor.

From relations (22) and (23) in the case $\delta > 1$, the largest crack results to be larger than the body itself for sufficiently large scales (Figure 3), suggesting a complete separation of the body. This paradox theoretically

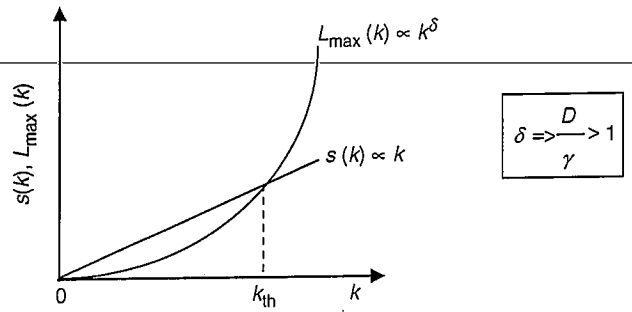


***Figure 3.*** *Trends of body size s and maximum defect size $L_{max}$ as functions of the scale in the case of defect size distribution with $\delta > 1$. This plot accounts for $\delta = 1$ as un upper limit to the values of $\delta$. For suitably small scales ($k < k_{th}$) the crack size distribution with $\delta > 1$ has physical meaning.*

accounts for $b_{crit} = 1$ as a lower limit to the $b$-values observed in most of AE monitoring tests on specimens loaded up to the failure (Colombo et al., 2003; Rao and Lakshmi, 2005; Carpinteri et al., 2006a). In fact, the conditions $D = 2$, i.e., damage concentrated over the through-going fracture surface, and $\delta = 1$, i.e., the largest crack proportional to the characteristic size of the structure, are both reached at the collapse (Carpinteri et al., 2006a; Carpinteri et al., 2007).

Till now no particular assumption has been made about $\gamma$, which in principle may take any value greater than 1. In reality, values smaller than 2 should not be allowed, since $b$ usually does not drop below 1 Equation (20). Nevertheless, for suitably small values of $k$, i.e., for sufficiently small bodies, condition $L_{max}(k) < s(k)$ is still satisfied. Hence crack-size distributions with $1 < \gamma < 2$ are physically admissible for reduced values of $k$ (Carpinteri et al., 2006a; Carpinteri et al., 2007). In terms of $b$-value, the condition $1 < \gamma < 2$ reads $1/2 < b < 1$, which have been observed in some AE tests (Colombo et al., 2003).

As a matter of fact, one way of reducing $k$ is to hold together a body through confining pressures or structural reinforcements in order to continue the test after fragmentation (Carpinteri et al., 2006b). That would mean a split of the initial one-body system in a multi-body system, characterized by reduced scaling factors $k'$, $k''$, $k'''$, etc. (Figure 4(a)). Scaling reduction below a threshold $k_{th}$ makes meaningful distributions with

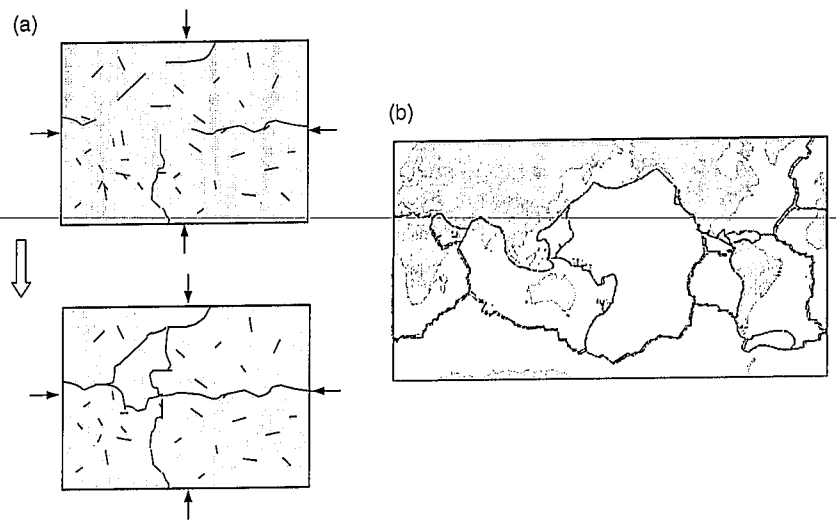


***Figure 4.*** *Similarity in fragmentation of a structure into multi-body system on different scales, from laboratory specimen (a) to Earth's crust (b).*

$1<\gamma<2$ (Figure 3), corresponding to observed $b$-values between 1/2 and 1 (Carpinteri et al., 2007).

It is possible, therefore, to conclude that $\gamma=2$ corresponds to $b_{crit}=1$ usually observed both in AE laboratory tests and in tests performed on full-sized engineering structures during main crack propagation (Colombo et al., 2003; Rao and Lakshmi, 2005; Carpinteri et al., 2006a; Carpinteri et al., 2007). In the light of the previous discussion, $b$-values in the range (1/2, 1) could be associated with fragmentation. The fragmentation of a structure seems to reproduce, on strongly reduced scale, the outline proposed by the Theory of Plate Tectonics, where the Earth's surface is broken into large plates moving against each other (Figure 4(b)). The $b$-value analysis emphasizes the analogy between these two multi-body systems, since in both cases $b$-values in the range $1/2<b<1$ can be observed (Schorlemmer, 2005; Carpinteri et al., 2007).

**Power-law Distributions and Fractal Dimensions**

The sole knowledge of the fractal dimension $D\equiv D_0$ of microcrack barycenters pattern is not sufficient to fully characterize the fractal geometry of a microcrack network. As said in the section 'Generalized fractal dimensions' a fractal object is characterized by an infinite set of generalized dimensions $D_q$, with $D_0\geq D_1\geq D_2\geq\cdots$ called the multifractal spectrum (Feder, 1988; Falconer, 1990; Bonnet, 2001). The multifractal spectrum fully characterizes the distribution of a measure on a geometric support; more precisely, it characterizes the level of regularity and homogeneity of the distribution. The dimension $D_0$ of the multifractal spectrum is the dimension of the geometric support, which can be either fractal or not. Here the geometric support is given by the ensemble of the microcrack barycenters, whereas the measure is the cumulative length of microcracks.

The box-counting method, in which all $d$-mesh boxes intersecting the microcrack barycenters pattern are counted, does not emphasize any fractal structure when applied to the crack length distribution of self-affinity modeled in the section 'From self-affinities to power-law distributions'. In fact, since all $N(d)\propto d^{-3}$ $d$-mesh boxes must be counted, the dimension $D_0$ of the crack barycenters pattern can be obtained from Equation (5):

$$D_0=-\lim_{d\to o}\frac{\ln d^{-3}}{\ln d}=3, \tag{24}$$

which agrees with the assumed homogeneous distribution for microcrack barycenters. It is worth noting that the result of Equation (21) can also be obtained from the generalized definition of fractal dimension (Feder, 1988).

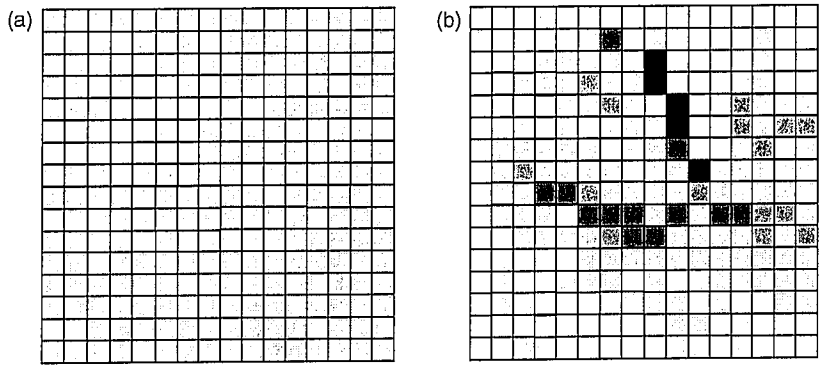


***Figure 5.*** *Classical methods used to calculate the fractal dimension applied to Carpinteri's model (1994) of self-affinity for microcrack network. The box-counting method equally counts microcracks irrespective of their length (a) the multifractal analysis weights each box by its total 'crack length'. The darker the box, the greater the crack length found inside it (b).*

However, as said above, the sole $D_0$ does not characterize the geometry of a crack network, which can be fractal even if its geometric support is not (Figure 5(a)). In order to emphasize the fractal structure subtended by the crack length distribution of self-affinity, a modified box-counting method is proposed, alternatively to the multifractal analysis pictured in Figure 5(b).

In line with the box-counting method proposed, $N(d)$ is taken to be the minimum number of balls of radius $d$ necessary for covering the microcrack network. As previously stated, fundamental to definition of dimension based on Equation (14) is the idea of 'measurement at scale $d$'. For each $d$, the set is measured in a way that ignores irregularities of size less than $d$ (Feder, 1988; Falconer, 1990; Carpinteri, 1994b). The number $N(d)$ of balls of radius $d$ that cover the microcrack net is an indication of how spread out or irregular the net is when examined at scale $d$.

The idea is that the number of balls necessary to cover at scale $L$ a microcrack network will be equal to the number $N(\geq L)$ of sampled microcracks (those having length $\geq L$), while irregularities, i.e., the microcracks, of size less than $L$ are ignored. Balls are centered on microcrack barycenters. In line with the approach followed by Bour and Davy (1999), the ball radius is defined as the average distance $d(L)$ between any crack of length $L$ and its nearest neighbor of length $L' \geq L$, so Equation (15) is unchanged.

Applying the self-affinity relation $L_{\max}(s) \propto s^{\delta}$ to a ball of radius $d(L)$ centerd on its largest crack $L$ gives (Figure 6):

$$d(L) \propto L^{1/\delta}. \tag{25}$$

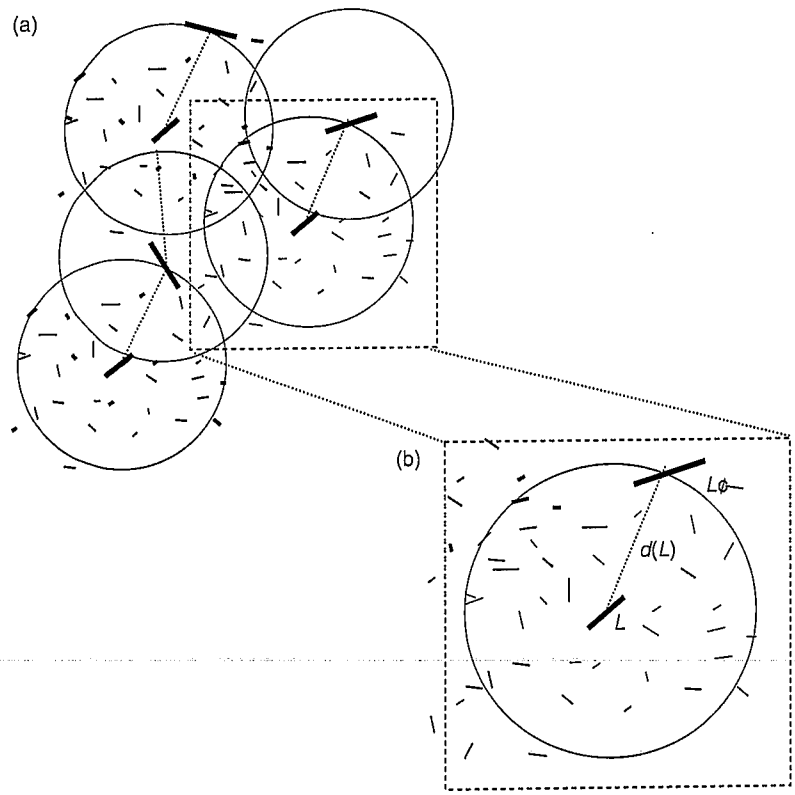


***Figure 6.*** *Balls used to cover the crack network at scale L(a). Zoom of one ball centered on its largest crack L, whose radius d(L) scales with L as $L^{1/\delta}$: the radius is determined by the nearest neighbor of length $L' \geq L$(b).*

Inserting Equation (25) into (7) gives:

$$N(\geq L) \propto L^{-D/\delta}. \tag{26}$$

A comparison with Equation (19) gives:

$$D = \gamma\delta. \tag{27}$$

Thus, we obtain again Equation (16) which now acquires a clear geometric meaning. In fact, a fractal network implies a spatial correlation and organization between cracks, which is independent of the distributions of other crack features, such as crack, lengths. In other words, cracks may be randomly distributed in space (i.e., nonfractal) while crack lengths can follow power law distributions. The link between the length distribution and the

(fractal) spatial distribution involves a relationship between the length of a crack and the distance to its neighbors, according to Bour and Davy (1999). In this light, the scaling law given by Equation (33) describes a distribution of cracks hierarchically organized in space: the larger the cracks, the larger their mutual distances. Physically, $d(L)$ helps to define a sort of excluded volume surrounding any crack with length $L$ such that no further crack with the same length (or greater) are admitted (Bour and Davy, 1999).

Let us note that a similar power-law scaling behavior has been observed studying the earthquake distributions (Caneva and Smirnov, 2004): after an earthquake had occurred in a certain region of space, there is a certain rank of energy values such that no further earthquake with the same energy can occur during a suitable interval time. The size $R$ of this prohibited region scales with the linear $l_0$ size of the earthquake rupture according to a power law, $R \propto l_0^{\alpha}$.

Furthermore, it is interesting to compare Equations (16) and (20) with analogous relationships recently proposed and based on the fragmentation model (Aki, 1981; Turcotte, 1997; Carpinteri and Pugno, 2002; Carpinteri et al., 2004):

$$D = \gamma = 2b, \tag{28}$$

and:

$$W \propto V^{D/3}, \quad \text{with} \quad 2 < D < 3. \tag{29}$$

The dissipation of energy $W$ on a fractal domain suggested by Equation (29) found experimental validation in crushing tests on concrete specimens (Carpinteri et al., 2004; Lacidogna and Carpinteri, 2006).

Equation (28) fails for high $b$-values (i.e., $b > 1.5$) often characterizing the early stages of the damage process (Rao and Lakshmi, 2005), since it gives values greater than 3 whose interpretation in terms of fractal dimension $D$ of the damage domain is problematic. Whereas, Equations (16) and (20) give $D = 2b\delta$, implying $D \leq 2b$ in light of the previous discussion see Equations (22) and (23), which still permits a consistent geometric interpretation of $D$ for high $b$-values.

We briefly discuss $b$-values in the range $0.5 < b < 1$, for which the fractal dimension becomes between 1 and 2. In this case one can imagine the microcracks trying to fill up a surface. Cracks propagate until they meet another crack or a boundary of the specimen. With proper boundary conditions fragments can be thus formed, which are defined as closed parts surrounded by intersected cracks. Therefore, a fractal dimension $D = 1$ (corresponding to $b$-values near 0.5 or lower) may be interpreted as describing the rupture propagation along a line given by

two intersecting rupture surfaces during a fracture process which evolves toward fragmentation.

Eventually, it is worth observing that in the present treatment we consider cracks and micro-cracks as the only possible defect type. Thus, voids, micro-voids, or other defects are not taken into consideration; at present, we made no attempt to investigate other types of defects, for which a fractal dimension could not be easily calculated with the proposed method, since it relies upon the crack size only, determined through AE analysis. In the case of damaged surfaces consisting primarily of voids or of a combination of cracks and voids (Ju and Chen, 1992), the proposed method needs to be further extended.

## EXPERIMENTAL ASSESSMENT: CONCRETE SPECIMEN IN COMPRESSION

The behavior of a concrete specimen in compression during a laboratory test has been investigated through AE monitoring. Six AE transducers ($S_{AE}$) have been applied to the surface of the specimen, a prism measuring $160 \times 160 \times 500\,mm^3$ (Figure 7). The test has been performed in displacement control by an electronic controlled Servo-hydraulic Material Testing Systems machine (311,31 model) with a capacity of 1800 kN, imposing a constant rate of displacement equal to $1 \times 10^{-4}$ mm/s to the upper loading platen. This kind of machine is controlled by an electronic closed-loop servo-hydraulic system. It is, therefore, possible to perform tests under load or displacement control. The displacements are recorded by four strain gauges (HBM 1-LY41-50/120 model) applied on the specimen surface. In spite of the low value chosen for the displacement rate, the specimen has failed in a brittle manner as it can be seen in the load versus time (strain) diagram of Figure 8, where the linear branch extends over almost the entire duration of the test.

The characterization of the fracture process through analysis of AE signals emerging from the growing cracks has been performed in a post processing environment, using two different procedures. In fact, besides the AE source location procedure already utilized in Carpinteri et al. (2005), the damage process has been evaluated through the *b*-value analysis. Both procedures make it possible to evaluate the dimension $D$ of the damaged domain, i.e., the fractal dimension of the crack network. The technique used to obtain a fractal dimension $D$ from the AE source location procedure is the two-point correlation function, which describes the spatial distribution of cracks, regarded as point-like, as often made in spatial characterization of crack networks (Okubo and Aki, 1987). This idealization is also convenient

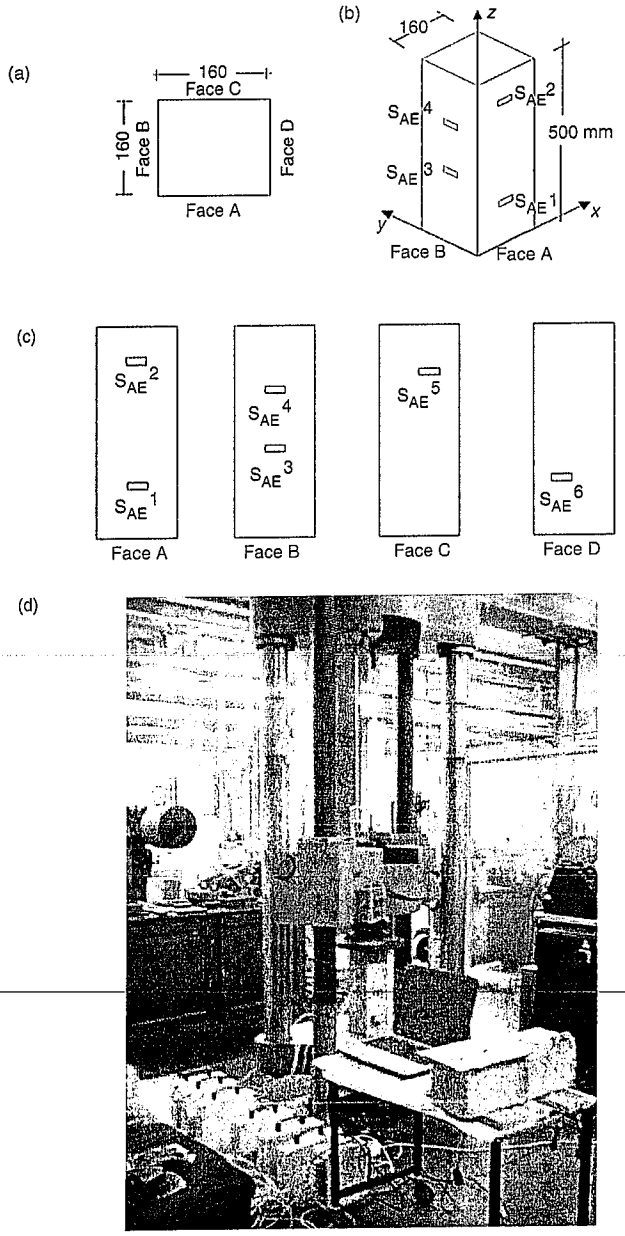


***Figure 7.*** *Concrete specimen in compression. (a) Cross section of the specimen. (b) Assonometric projection with the positioned AE sensors. (c) Overview of the four specimen faces. (d) Photo of MTS machine and of the specimen during the test. Note on the left the devices utilized for detection of AE signals.*

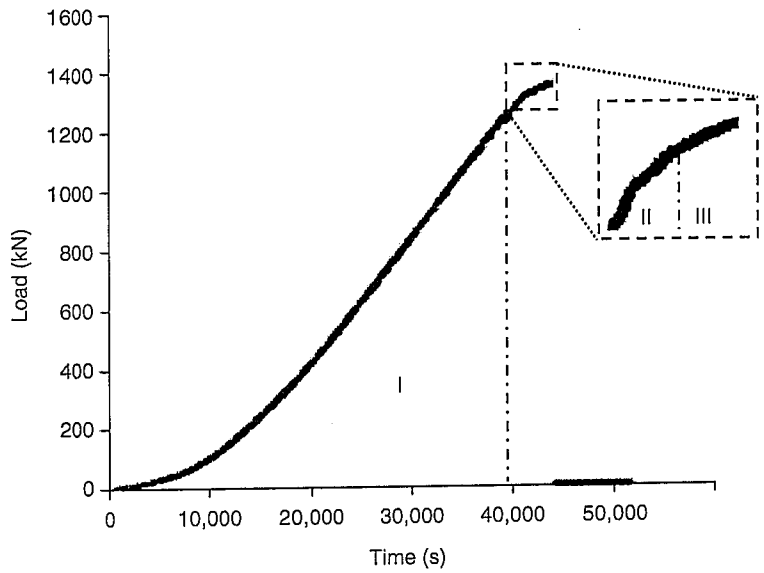


***Figure 8.*** *Load-time diagram of the test performed in displacement control: in the first $10^4$ s the displacement rate was $d\delta/dt = 10^{-5}$ mm/s, increased to $10^{-4}$ mm/s from $t = 10^4$ s up to failure. The specimen failed in a quasi-brittle manner, in region I, where linear elasticity is applicable, there is little damage (i.e., low-amplitude AE events), while in regions II and III, damage results in a deviation from linear elasticity and an increase of AE level.*

for a comparison with data from AE localization of sources, in which events of all different magnitudes are localized as if they were point-like.

In general the two-point correlation function $C(d)$ gives the probability that two points are less than $d$ apart. To compute this probability for any given value of the distance $d$, the number of pairs of cracks closer than $d$ must be evaluated and then divided by the total number of crack couples. Given $N$ cracks, the total number of crack pairs is given by $N(N-1)/2$. The number of pairs closer than $d$ is computed as follows: given two cracks $i$ and $k$, the Heaviside step function $\Theta(d - |\mathbf{x}_k - \mathbf{x}_j|)$ ($\Theta(x) = 1$ if $x > 0$, and zero elsewhere) provides 1 if the cracks are closer than $d$ and 0 otherwise. By performing a double sum of over the indexes $i$ and $k$, we obtain the number:

$$C(d) \equiv \frac{2}{N(N-1)} \sum_{k=1}^{N-1} \sum_{j=k+1}^{N} \Theta(d - |\mathrm{x}_k - \mathrm{x}_j|). \tag{30}$$

Therefore, taking a crack in $\mathbf{x}_i$, $C(d)$ gives thus the probability of finding another crack in the sphere of radius $d$ centered at $\mathbf{x}_i$. The correlation

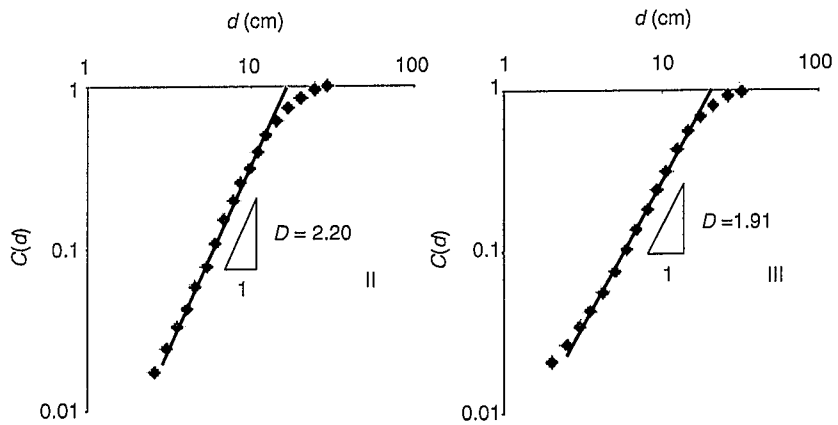


***Figure 9.*** *Correlation function–distance diagram illustrated in the last two stages of the loading test, when the two-point correlation algorithm was applicable. The fractal dimension D, calculated by the Equation (39), is the slope of the function on the log-log plot.*

function can then be used to calculate the fractal dimension of the population of cracks by using the scaling relation:

$$C(d) \propto d^D. \tag{31}$$

Note that the correlation dimension $D$ is equivalent to the generalized fractal dimension $D_2$ (Feder, 1988), but easier to calculate (Grassberger and Procaccia, 1983). In fact, the probability $\Sigma\mu_i^2$ of finding two points in a cell with side $d$ (being $\mu_i$ is the probability of finding one point in a $i$th specific cell) is nearly the same as in a circle with radius $d$:

$$\sum_i \mu_i^2 \cong C(d). \tag{32}$$

By varying the value for $d$, a plot has been made to represent the changing value of the correlation function vs. the distance $d$. The correlation dimension $D$ is then the slope of the function on the log-log plot. The graph of $C(d)$ at two different stages of the damage process is shown in Figure 9. The curves show a linear behavior in a range of about one order of magnitude on the space scale (i.e., from ~1 cm to ~10 cm). Deviations from linear dependence in the range of wider scales are connected with the finite size of the specimen. It turns out that at earlier stages of the damage process $D$ reaches the value of 2.20, which describes microcracks trying to fill up the specimen volume $V$, consistently with the idea of diffused microcracking at the early stages of damage.

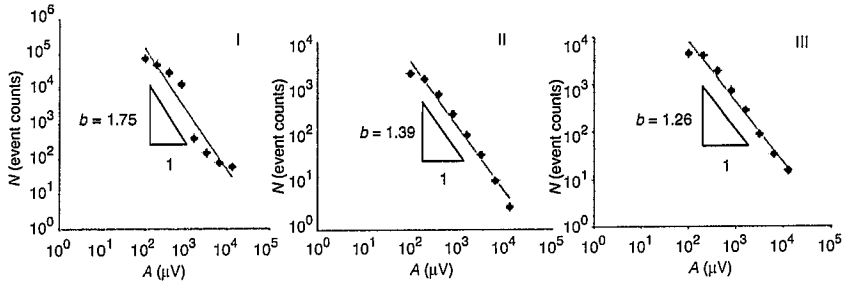


*Figure 10. b-values during the three stages of the loading test, obtained illustrating the GR law: $N(\geq A) \propto A^{-b}$, in which the b-value is the negative slope of the number of AE events with signal amplitude greater than A as a function of A on the log-log plot.*

***Table 1. Parameters characterizing the crack network at different stages of damage evolution: b-value defining the crack-length distribution, fractal dimension D of the crack barycenters (obtained from two-point correlation algorithm), and exponent $\delta$ defining the excluded volume surrounding any crack.***

| Damage stage | I | II | III |
|---|---|---|---|
| $b$ | 1.75 | 1.39 | 1.26 |
| $D$ | (*) | 2.20 | 1.91 |
| $\delta = D/(2b)$ | | 0.79 | 0.76 |

(*) Two-point correlation algorithm not applicable due to lack of localized points.

During the evolution of the process, $D$ decreases reaching a value of 1.91 before the rupture, signifying that at the final stage microcracks tend to be localized on the through-going fracture surface.

The same temporal partition used for the correlation dimension has been used for calculating the $b$-values, obtaining, respectively, 1.39 and 1.26 (Figure 10); as expected, both $D$ and $b$ share the same decreasing trend as the damage develops. By resorting to Equation (16) we can compute the value of the exponent $\delta$, obtaining 0.79 and 0.76 in phases II and III, respectively Table 1. Such values of $\delta$ have been compared with the related experimental value, obtained by subjecting the AE data to a statistical analysis: exploiting the scaling relation existing between the peak amplitude $A$ of a recorded AE signal and the length $L$ of the crack source, $L \propto A^{1/2}$ (Colombo et al., 2003; Carpinteri et al., 2007), and inserting it into Equation (33), we obtain the distance $d$ between the localized cracks as a function of the related AE signal amplitudes, $d(A) \propto A^{1/2\delta}$. Plotting $d(A)$ versus $A$ according to a simple

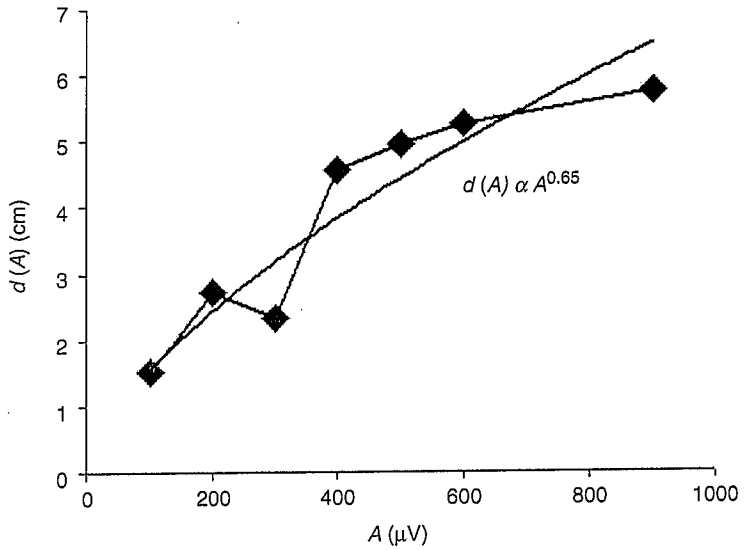


***Figure 11.*** *Plot of the average distance d(A) between a crack of length $L \propto A^{1/2}$ and its nearest neighbor having a length $\geq L$ vs A. d(A) is fitted by $d(A) \propto A^x$ with $x = 0.65$.*

power-law, we have found an exponent $x = 1/2\delta = 0.65$ Figure 11 corresponding to an experimental value of $\delta \cong 0.77$, which is in good agreement with the values previously calculated by Equation (16) (Table 1).

Furthermore, the *b*-value has been calculated also at the earliest stage of the loading test, where linear elasticity was still applicable, obtaining a value of 1.75, index of low damage level (Figure 10). Therefore, during the evolution of damage process, the *b*-value progressively decreases as expected.

In the linear regime, the recorded low-amplitude AE signals have not allowed the location of microcracks (an AE event must be detected by at least two transducers for crack location), then neither the calculation of the correlation dimension. It is worth noting the consistency of this experimental evidence, since both the deviation from linear elasticity and the AE are traced back to the phenomenon of damage. The localization of both these aspects of damage in a narrow time window before the rupture is a typical example of brittle behavior exhibited by the specimen. A final overview of the localized AE crack sources overlapped to the fracture surfaces is illustrated in Figure 12. It might be observed that in the Figure 12 two different clusters of cracks are visible. All the data are fitted with just one line and not separately, since the *b*-values of the two clusters of AE events have a very similar evolution in time. As a matter of

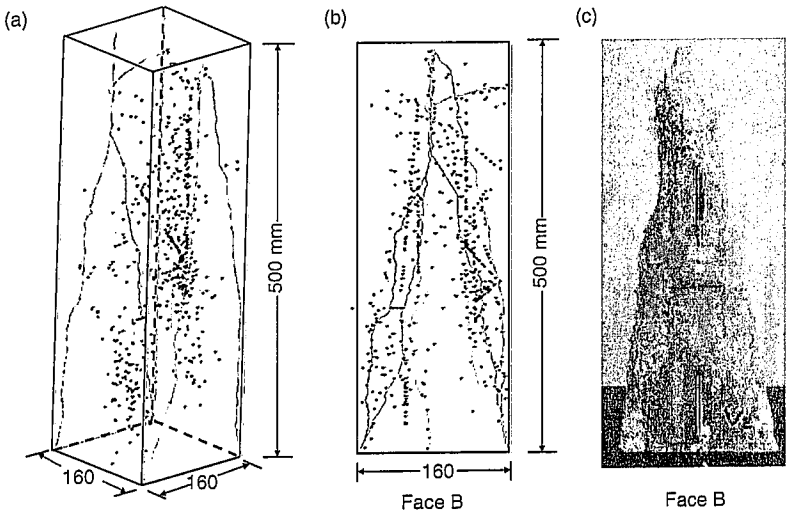


***Figure 12.*** *Concrete specimen in compression. (a) Final overview of the localized AE crack sources overlapped to the fracture surfaces. (b) FACE B with the projections of the AE sources and fracture surfaces identified during the loading test. (c) Broken specimen after testing from FACE B.*

fact, although clearly distinguishable, the two cracks proceed from the same damage process and evolve in a similar way.

## CONCLUSIONS

Assuming a relation of self-affinity for microcracks, $L_{max}(s) \propto s^{\delta}$, we show that the fractal dimension $D$ and the exponent $\gamma$ of the frequency length distribution of a crack network are related through the relation $D = \delta\gamma$, where $\delta$ is the governing exponent of the hierarchical organization of cracks in space. Likewise an analogous scaling behavior for the spatial distribution of hypocenters, is observed studying the seismic recurrence. The link with the experiments is provided by another relation foreseen by the model, $\gamma = 2b$, which permits to study the geometry of a crack network through AE tests. The proposed relation, $D = \delta\gamma$, holds a physical significance in terms of spatial distribution of damage even for high (i.e., >1.5) $b$-values.

Furthermore, besides the fractal features of a crack network, the model provides a theoretical explanation for taking $b_{crit} = 1$ as a lower limit to the $b$-values, as observed in most of AE monitoring tests on specimens loaded up to failure. Interpretation in terms of fragmentation for $b$-values lower than 1, intriguingly suggested by the outline of the Theory of Plate Tectonics and the earthquake statistics, is worthy of further investigations.

## ACKNOWLEDGMENTS

This research was carried out with the financial support of the Ministry of University and Scientific Research (MIUR) and of the European Union (EU) Leonardo da Vinci Programme, ILTOF Project.

## REFERENCES

Aki, K. (1981). A Probabilistic Synthesis of Precursory Phenomena in Earthquake Prediction, In: Simpson, D.W. and Richards, P.G. pp. 566–574, American Geophysical Union, Washington.

Bonnet, E., Bour, O., Odling, N.E., Davy, P., Main, I., Cowie, P. and Berkowitz, B. (2001). Scaling of Fracture Systems in Geological Media, *Reviews of Geophysics*, 3: 347–383.

Bour, O. and Davy, P. (1999). Clustering and Size Distributions of Fault Patterns: Theory and Measurements, *Geoph. Res. Lett.*, **13**: 2001–2004.

Bour, O., Davy, P., Darcel, C. and Odling, N. (2002). A Statistical Scaling Model for Fracture Network Geometry, with Validation on a Multiscale Mapping of a Joint Network (Hornelen Basin, Norway), *Journal of Geophysical Research*, **107**: 2001JB000176.

Caneva, A. and Smirnov, V. (2004). Using the Fractal Dimension of Earthquake Distributions and the Slope of the Recurrence Curve to Forecast Earthquakes in Colombia, *Earth Sciences Research Journal*, **8**: 3–9.

Carpinteri, A. (1986). *Mechanical Damage and Crack Growth in Concrete: Plastic Collapse to Brittle Fracture*, Martinus Nijhoff Publishers, Dordrecht.

Carpinteri, A. (1989). Decrease of Apparent Tensile and Bending Strength with Specimen Size: Two Different Explanations Based on Fracture Mechanics, *International Journal of Solids and Structures*, **25**: 407–429.

Carpinteri, A. (1994a). Scaling Laws and Renormalization Groups for Strength and Toughness of Disordered Materials, *International Journal of solids and structures*, **31**: 291–302.

Carpinteri, A. (1994b). Fractal Nature of Material Microstructure and Size Effects on Apparent Mechanical Properties, *Mechanics of Materials*, **18**: 89–101.

Carpinteri, A. and Pugno, N. (2002). One, Two, and Three-Dimensional Universal Laws for Fragmentation Due to Impact and Explosion, *Journal of Applied Mechanics*, **69**: 854–856.

Carpinteri, A., Lacidogna, G. and Pugno, N. (2004). Scaling of Energy Dissipation in Crushing and Fragmentation: a Fractal and Statistical Analysis Based on Particle Size Distribution, *International Journal of Fracture*, **129**: 131–139.

Carpinteri, A., Lacidogna, G. and Niccolini, G. (2005). Crack Localisation in a Large-Sized R.C. Beam Through the Acoustic Emission Technique, In: *Proc. of the 17th National Congress of Theoretical and Applied Mechanics* (AIMETA), Florence, CD-Rom, Paper No. 23.

Carpinteri, A., Lacidogna, G. and Niccolini, G. (2006a). Critical Behaviour in Concrete Structures and Damage Localization by Acoustic Emission, *Key Engineering Materials*, **312**: 305–310.

Carpinteri, A., Lacidogna, G. and Pugno, N. (2006b). Richter's Laws at the Laboratory Scale Interpreted by Acoustic Emission, *Magazine of Concrete Research*, **58**: 619–625.

Carpinteri, A., Lacidogna, G. and Niccolini, G. (2007). Critical Defect Size Distributions in Concrete Structures Detected by the Acoustic Emission Technique, *Meccanica*, **43**: 349–363.

Colombo, S., Main, I.G. and Forde, M.C. (2003). Assessing Damage of Reinforced Concrete Beam Using "*b*-value" Analysis of Acoustic Emission Signals, *Journal of Materials in Civil Engineering* ASCE, **15**: 280–286.

Davy, P., Sornette, A. and Sornette, D. (1990). Some Consequences of a Proposed Fractal Nature of Continental Faulting, *Nature*, **348**: 56–58.

Falconer, K. (1990). *Fractal Geometry*, J. Wiley & Sons, Chichester.

Feder, J. (1988). *Fractals*, Plenum Press, New York and London.

Grassberger, P. and Procaccia, I. (1983). Characterization of Strange Attractors, *Phys. Rev. Lett.*, **50**: 346–349.

Hausdorff, F. (1919). Dimension und Äusseres Mass, *Mathematische Annalen*, **79**: 157–179.

Ju, J.W. and Chen, T.M. (1992). Effective moduli of elastic composites containing microcracks or microvoids, In: D.H. Allen, and D.C. Lagoudas (ed.), *Damage Mechanics in Composites*, AMD-Vol. 150 and AD-Vol. 32, pp. 181–190, ASME Press, New York, Nov. 1992.

King, G. (1986). Speculations on the Geometry of the Initiation and Termination Processes of Earthquake Rupture and its Relation to Morphology and Geological Structure, *Pure Appl. Geophys.*, **124**: 567–585.

Krajcinovic, D. (1996). *Damage Mechanics*, Elsevier, Amsterdam.

Krajcinovic, D. and Rinaldi, A. (2005). Statistical Damage Mechanics - 1. Theory, *Journal of Applied Mechanics*, **72**: 76–85.

Lacidogna, G. and Carpinteri, A. (2006). Monitoring Durability Performances of Concrete and Masonry Structures by Acoustic Emission, *Fracture of Nano and Engineering Materials and Structures Proc. of the 16th European Conference of Fracture*, Alexandroupolis, Greece, 2006, Ed. E.E. Gdoutos, Springer, Dordrecht, CD-ROM, Paper N. 218.

Mandelbrot, B.B. (1982). *The Fractal Geometry of Nature*, W. H. Freeman, New York.

Newman, M.E.J. (2005). Power laws, Pareto distributions and Zipf's law. *Contemporary Physics*, **46**: 323–351.

Ohtsu, M. (1996). The History and Development of Acoustic Emission in Concrete Engineering, *Magazine of Concrete Research*, **48**: 321–330.

Okubo, P.G. and Aki, K. (1987). Fractal Geometry in the San Andreas Fault System, *J. Geophys. Res.*, **92**: 345–355.

Rao, M.V.M.S. and Lakshmi, K.J.P. (2005). Analysis of *b*-value and Improved *b*-value of Acoustic Emissions Accompanying Rock Fracture, *Current Science*, **89**: 1577–1582.

Rinaldi, A., Mastilovic, S. and Krajcinovic, D. (2006). Statistical Damage Mechanics - 2. Constitutive Relations, *Journal of Theoretical and Applied Mechanics*, **44**: 585–602.

Sammis, C.G., Osborne, R.H., Anderson, J.L., Banerdt, M. and White, P. (1986). Self-Similar Cataclasis in the Formation of Fault-Gouge, *Pure Appl. Geophys*, **123**: 53–78.

Sammis, C.G. and Steacy, S.J. (1995). Fractal Fragmentation in Crustal Shear Zones. In: Barton, C.C. and La Pointe R. (eds), *Fractals in the Earth Sciences*, Plenum Press, New York, pp. 179–204.

Sammonds, P.R., Meredith, P.G., Murrel, S.A.F. and Main, I.G. (1994). Modelling the damage evolution in rock containing porefluid by acoustic emission, *Proc. of Eurock'94*, Balkema, Rotterdam, The Netherlands.

Schorlemmer, D., Wiemer, S. and Wyss, M. (2005). Variations in Earthquake-Size Distribution Across Different Stress Regimes, *Nature*, **348**: 539–542.

Turcotte, D.L. (1986). A Fractal Model for Crustal Deformation, *Tectonophysics*, **132**: 261–269.

Turcotte, D.L. (1997). *Fractals and Chaos in Geology and Geophysics*, Cambridge University Press, Cambridge.